

# Bayesian Masking: Sparse Bayesian Estimation with Weaker Shrinkage Bias

Yohei Kondo  
Shin-ichi Maeda

*Graduate School of Informatics, Kyoto University, Kyoto, Japan*

YKONDO@SYS.I.KYOTO-U.AC.JP

ICHI@SYS.I.KYOTO-U.AC.JP

Kohei Hayashi

*National Institute of Informatics, Tokyo, Japan*

HAYASHI.KOHEI@GMAIL.COM

## Abstract

A common strategy for sparse linear regression is to introduce regularization, which eliminates irrelevant features by letting the corresponding weights be zeros. Regularization, however, often shrinks the estimator for relevant features, which leads incorrect feature selection.

Motivated by the above issue, we propose a sparse estimation method—Bayesian masking (BM)—that imposes no regularization on the weights. The key concept of BM is to introduce binary latent variables that randomly mask features. Estimating the masking rates determines the relevances of the features automatically. We derive a variational Bayesian inference algorithm that maximizes a lower bound of the factorized information criterion (FIC), which is a recently-developed asymptotic evaluation of the marginal log-likelihood. We also propose reparametrization that accelerates the convergence. We demonstrate that BM outperforms Lasso and automatic relevance determination (ARD) in terms of the sparsity-shrinkage trade-off.

**Keywords:** Sparse estimation, Factorized information criterion, Lasso, Automatic relevance determination

## 1. Introduction

In sparse linear regression, various approaches impose sparsity by implementing regularization for a weight parameter. For example, Lasso (Tibshirani, 1994) introduces the sparsity by regularizing the weights by L1 norm. Automatic relevance determination (ARD) (MacKay, 1994; Neal, 1996) regularizes the weights by a prior distribution with hyperparameters indicating the relevance of input features. Empirical Bayes estimation of the hyperparameters thus eliminates irrelevant features automatically. Although ARD is notorious for slow convergence, several authors improved the algorithm (e.g. (Wipf and Nagarajan, 2008)).

The trade-off between sparsity and shrinkage is a crucial issue in sparse regularization methods (Aravkin et al., 2014). In Lasso, for example, a large regularization constant incorporates strong sparsity and more likely to estimate the weights of irrelevant features as zero, which is desirable in terms of the interpretability. However, it also shrinks the weights of relevant features and may eliminate them. ARD has the same problem, though the bias of ARD is weaker than the bias of Lasso (Aravkin et al., 2014). Because both

sparsity and shrinkage are caused by regularization, the shrinkage effects are inevitable as long as we use the regularization scheme.

To address this issue, we propose an alternative method for sparse estimation, Bayesian masking (BM), which is distinguished from the existing methods by not imposing any regularization on the weights. Our contributions are highlighted as follows.

- The BM model (section 4). The BM model introduces binary latent variables to a linear regression model. The latent variables randomly masks features to be zero at each sample, according to the priors which are defined for each feature, but shared between samples. The estimation of the priors on masking rates determines the relevance of the features.
- A variational Bayesian inference algorithm for the BM model (section 4.2). The EM-like coordinate ascent algorithm maximizes a lower bound of the factorized information criterion (FIC). The convergence is accelerated by combining gradient ascent and reparametrization (section 4.4) that are motivated by previous studies about the convergence analysis of coordinate ascent and information geometry.
- Analytic forms of the one-dimensional (1D) estimators of Lasso, ARD (section 3), and BM (section 4.3). The analytic estimators provide intuitions about their shrinkage mechanisms.

In numerical experiments, we empirically show that our proposed method outperforms Lasso and ARD in terms of the sparsity-shrinkage trade-off.

## 1.1. Notation

Hereafter,  $\mathbf{x}_n$  and  $\mathbf{x}_k$  denote column vectors of the  $n$ -th row and the  $k$ -th column of a matrix  $X$ , respectively.

## 2. Background

### 2.1. Linear Regression and Least Squares

Consider a linear regression model:

$$\mathbf{y} = X\boldsymbol{\beta} + \boldsymbol{\epsilon}, \tag{1}$$

where  $\mathbf{y} \in \mathbb{R}^N$  is a vector of target values,  $X \in \mathbb{R}^{N \times K}$  is a matrix of explanatory variables,  $\boldsymbol{\beta} \in \mathbb{R}^K$  is a vector of weight parameters, and  $\boldsymbol{\epsilon} \sim N(0, \lambda^{-1}I)$  is observation noise;  $N$  is the number of samples and  $K$  is the number of features. Because the noise is i.i.d. Gaussian, the maximum likelihood estimator (MLE) is given as the least squares (LS) solution:

$$\hat{\boldsymbol{\beta}}_{\text{LS}} = \arg \min_{\boldsymbol{\beta}} \frac{\lambda}{2} \|\mathbf{y} - X\boldsymbol{\beta}\|_2^2 = (X^\top X)^{-1} X\mathbf{y}. \tag{2}$$

## 2.2. Lasso

Lasso is formulated as the L1-penalized regression problem, and the estimator is given as

$$\hat{\boldsymbol{\beta}}_{\text{Lasso}} = \arg \min_{\boldsymbol{\beta}} \frac{\lambda}{2} \|\mathbf{y} - X\boldsymbol{\beta}\|_2^2 + \alpha \|\boldsymbol{\beta}\|_1, \quad (3)$$

where  $\alpha (> 0)$  is a regularization constant.

## 2.3. ARD

Consider the prior distribution of  $\boldsymbol{\beta}$ :

$$p(\boldsymbol{\beta}|\boldsymbol{\gamma}) = N(\boldsymbol{\beta}|0, \Gamma) \quad (4)$$

where  $\Gamma = \text{diag}(\boldsymbol{\gamma})$  and  $\boldsymbol{\gamma}$  is the hyperparameter determining the variance of the prior. ARD determines  $\boldsymbol{\gamma}$  by the empirical Bayes principle, i.e., maximizing the marginal log-likelihood:  $\hat{\boldsymbol{\gamma}} = \arg \max_{\boldsymbol{\gamma}} \int p(\mathbf{y}|\boldsymbol{\beta})p(\boldsymbol{\beta}|\boldsymbol{\gamma}, \lambda)d\boldsymbol{\beta}$ . The estimator of  $\boldsymbol{\beta}$  is then often given by the posterior mean with plugged-in  $\hat{\boldsymbol{\gamma}}$  (Wipf and Nagarajan, 2008; Aravkin et al., 2014), which is

$$\hat{\boldsymbol{\beta}}_{\text{ARD}} = \hat{\Gamma} X^\top (\lambda^{-1} I + X \hat{\Gamma} X^\top)^{-1} \mathbf{y}. \quad (5)$$

Clearly, for  $\lambda^{-1} > 0$ ,  $\hat{\gamma}_k = 0$  results in  $\beta_k = 0$  for any  $k$ .

## 3. The Trade-off between Sparsity and Shrinkage

Concerning the trade-off between sparsity and shrinkage, Aravkin et al. (2014) derive the upper-bounds of the estimators for  $K = 2$  and show that undesirable shrinkage occurs for both Lasso and ARD; specifically, the shrinkage bias of Lasso is larger than that of ARD under the condition that the unnecessary feature is correctly pruned.

In this section, we revisit this issue. To understand how sparse regularization works, we derive the exact forms of the estimators for  $K = 1$  and show that ARD is better than Lasso in terms of the sparsity-shrinkage trade-off. Although our analysis is much simpler than the earlier study by Aravkin et al. (2014), it is still meaningful because our derived estimators

- are exact and analytically written (no approximation is needed) and
- highlight the substantial difference between ARD and Lasso.

### 3.1. 1D Estimators

**LS** When  $K = 1$ , the matrix inverse in eq. (2) becomes a scalar inverse and  $\hat{\beta}_{\text{LS}}$  is simply written as

$$\hat{\beta}_{\text{LS}} = \frac{\mathbf{x}^\top \mathbf{y}}{\mathbf{x}^\top \mathbf{x}}. \quad (6)$$

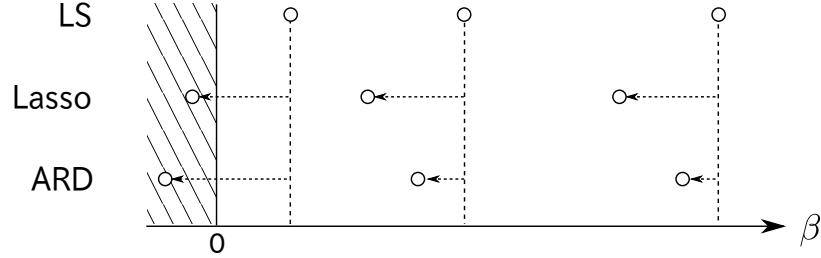


Figure 1: The illustrative comparison of the shrinkage effect with Lasso and ARD in the 1D case. Lasso shifts the estimator to zero by the same value, whereas ARD shrinks larger when the LS estimator is smaller.

**Lasso** For  $\beta \geq 0$ , the L1-penalty becomes  $\alpha\beta$ . Putting this into eq. (3) yields an stationary point  $\hat{\beta}_{\text{LS}} - \alpha/\mathbf{x}^\top \mathbf{x}$  where  $\hat{\beta}_{\text{LS}} = \mathbf{x}^\top \mathbf{y}/\mathbf{x}^\top \mathbf{x}$ . For  $\beta < 0$ , the solution is the same except the sign is flipped. Combining them yields the solution for all  $\beta$ :

$$\hat{\beta}_{\text{Lasso}} = \text{sign}(\hat{\beta}_{\text{LS}}) \max(0, |\hat{\beta}_{\text{LS}}| - \frac{2\alpha}{\lambda \mathbf{x}^\top \mathbf{x}}) \quad (7)$$

**ARD** Similar to Lasso, the 1D estimator of ARD is analytically written as<sup>1</sup>

$$\hat{\beta}_{\text{ARD}} = \text{sign}(\hat{\beta}_{\text{LS}}) \max(0, |\hat{\beta}_{\text{LS}}| - \frac{1}{\lambda |\mathbf{x}^\top \mathbf{y}|}). \quad (8)$$

Note that we assumed  $\lambda$  is known.<sup>2</sup>

### 3.2. Comparison between LS, Lasso and ARD

While the regularizations are different, Lasso and ARD have the same shrinkage mechanism — subtracting the constant from  $\hat{\beta}_{\text{LS}}$  and cropping  $\hat{\beta}_{\text{LS}}$  to zero if the magnitude is smaller than the constant. Since the constants in eqs. (7) and (8) are both larger than zero except for the noiseless case (i.e.,  $\lambda = \infty$ ), the shrinkage bias is inescapable in both Lasso with  $\alpha > 0$  and ARD. On the other hand, this retraction to zero is necessary for the sparsity because it prunes the irrelevant features.

It is worth noting that the bias of ARD is much weaker than Lasso when the scale of  $\hat{\beta}_{\text{ARD}}$  is large. This is easily confirmed by transforming the constant in eq. (8) as  $(\lambda |\mathbf{x}^\top \mathbf{y}|)^{-1} = (\lambda \mathbf{x}^\top \mathbf{x} |\hat{\beta}_{\text{LS}}|)^{-1}$ , indicating that the shrinkage is weak when  $|\hat{\beta}_{\text{LS}}|$  is large, but the shrinkage is strong when  $|\hat{\beta}_{\text{LS}}|$  is close to zero. Compared to Lasso, this behavior of ARD is desirable, which enables to maintain sparsity for weak features while alleviating unnecessary shrinkage. Figure 1 illustrates how shrinkage occurs in Lasso and ARD.

1. The full derivation of eq. (8) is shown in Appendix A.

2. Practically,  $\lambda$  is set to the unbiased version of MLE (Aravkin et al., 2014).

## 4. The BM Model and The Inference Algorithms

### 4.1. The BM Model

Obviously, the shrinkage bias of Lasso and ARD comes from their regularizations on the weights. For example, if  $\alpha = 0$  in Lasso, the loss function becomes equivalent to that of LS, and of course, no shrinkage occurs. Using  $\gamma = \infty$  yields the same result in ARD.

Hence we introduce a new estimation method, which keeps sparsity by latent variables instead of regularization. Let  $Z \in \{0, 1\}^{N \times K}$  be binary latent variables having the same dimensionality of  $X$ . We insert  $Z$  between  $X$  and  $\beta$ , namely

$$\mathbf{y} = (X \circ Z)\beta + \epsilon, \quad (9)$$

where ' $\circ$ ' denotes the Hadamard product (i.e., element-wise multiplication).

$Z$  masks the features randomly at each sample. For a Bayesian treatment, we introduce prior distributions. We assume that  $Z$  follows a Bernoulli prior distribution as  $z_{nk} \sim \text{Bern}(\pi_k)$ , where  $\pi_k$  represents how feature  $k$  is relevant. Then, estimating the priors on the masking rates automatically determines the relevances of the features.

We also introduce the priors for  $\beta$  and  $\lambda$ ; however, we set them as weak as possible such that their effects are ignorable when  $N$  is sufficiently large. Thus, we just put them as constant as it does not depend on  $N$ , i.e.,  $\log p(\beta, \lambda) = O(1)$ .

### 4.2. The FAB-EM Algorithm

Our approach is based on the idea of Bayesian model selection, and then the central task is to evaluate the marginal log-likelihood. However, in our case, the marginal likelihood is intractable.

Thus, we adopt FIC, a recently proposed approximation for the marginal log-likelihood (Fujimaki and Morim 2012; Hayashi and Fujimaki, 2013; Hayashi et al., 2015). We also adopt the factorized asymptotic Bayesian inference (FAB), which provides a tractable algorithm for parameter inference and model pruning via optimizing a lower bound of FIC. A FAB algorithm alternately maximizes the lower-bound in an EM algorithm-like manner.

To obtain the lower-bound of FIC, we introduce a mean-field approximation on the posterior distribution of  $Z$  as  $q(z_n) = \prod_k q(z_{nk}) = \prod_k \text{Bern}(\mu_{nk})$ . Then we obtain the objective function as

$$\begin{aligned} \mathcal{G}(\{\mu_n\}, \beta, \lambda, \pi) &= \mathbb{E}_q[\log p(\mathbf{y}|X, Z, \beta, \lambda)] + \mathbb{E}_q[\log p(Z|\pi)] \\ &\quad - \frac{1}{2} \sum_k \left( \log(N\pi_k) + \frac{\sum_n \mathbb{E}_q[z_{nk}]/N - \pi_k}{\pi_k} \right) - \frac{K+1}{2} \log N \\ &\quad + \sum_{n,k} H(q(z_{nk})), \end{aligned} \quad (10)$$

where  $q = q(Z)$  is the posterior of  $Z$  and  $H$  is the entropy. The derivation of eq. (10) is described in Appendix B.

**FAB E-step** In the FAB E-step, we updates  $\{\mu_{nk}\}$ . By taking the gradient of  $\mathcal{G}$  w.r.t.  $\mu_{nk}$  and setting it to zero, we obtain the following fixed-point equations:

$$\mu_{nk} = \sigma \left( c_{nk} + \log \frac{\pi_k}{1 - \pi_k} - \frac{1}{2N\pi_k} \right) \quad (11)$$

where  $\sigma(\cdot)$  is the sigmoid function and  $c_{nk} = x_{nk}\beta_k\lambda(y_n - \frac{1}{2}x_{nk}\beta_k - \sum_{l \neq k} \mu_{nl}x_{nl}\beta_l)$ . Updates of eq. (11) several times give us  $\{\mu_{nk}\}$  at a local maximum of  $\mathcal{G}$ .

**FAB M-step** Since only the first and the second terms in eq. (10) are relevant, the FAB M-step is equivalent to the M-step in the EM algorithm. We have the closed-form solutions to update  $\beta$ ,  $\lambda$ , and  $\pi$  as

$$\beta = \Omega^{-1}(X \circ M)^\top \mathbf{y}, \quad (12)$$

$$\frac{1}{\lambda} = \frac{\sum_n (y_n^2 - 2y_n(\mathbf{x}_n \circ \boldsymbol{\mu}_n)^\top \beta + (\mathbf{x}_n \circ \beta)^\top \mathbb{E}_q[\mathbf{z}_n \mathbf{z}_n^\top] (\mathbf{x}_n \circ \beta))}{N} \quad (13)$$

$$\pi_k = \sum_n \frac{\mu_{nk}}{N}. \quad (14)$$

where  $\Omega = \sum_n (\mathbf{x}_n \mathbf{x}_n^\top) \circ \mathbb{E}_q[\mathbf{z}_n \mathbf{z}_n^\top]$  and  $M = (\boldsymbol{\mu}_1, \dots, \boldsymbol{\mu}_N)^\top$ . We note that  $\mathbb{E}_q[\mathbf{z}_n \mathbf{z}_n^\top] = \boldsymbol{\mu}_n \boldsymbol{\mu}_n^\top + \text{diag}(\boldsymbol{\mu}_n - \boldsymbol{\mu}_n \circ \boldsymbol{\mu}_n)$ .

**Pruning step** As noted in the previous papers, the third term in  $\mathcal{G}$  penalize  $\{\mu_{nk}\}$  and automatically eliminates irrelevant features. Then, when  $\pi_k = \sum_n \mu_{nk}/N < \delta$ , we remove the corresponding feature from the model. The resulting algorithm is shown in the pseudo-code in Algorithm 1.

---

**Algorithm 1** Bayesian masking by FAB-EM algorithm

---

- 1: Initialize  $(\{\boldsymbol{\mu}_n\}, \beta, \lambda, \pi)$
  - 2: **repeat**
  - 3:   Update  $\{\mu_{nk}\}$  by eq. (11)
  - 4:   **for**  $k = 1, \dots, K$  **do**
  - 5:     **if**  $\sum_n \mu_{nk}/N < \delta$  **then**
  - 6:       Remove  $k$ -th dimension from the model
  - 7:     **end if**
  - 8:   **end for**
  - 9:   Update  $(\beta, \lambda, \pi)$  by eqs. (12-14)
  - 10: **until** termination criterion is met
- 

### 4.3. Analysis on The FAB Estimator

As in section 3, we investigate the FAB estimator of  $\beta$ . If  $\mathbf{y}$  follows the linear model (1) with  $\beta = \beta^*$ , the FAB estimator is expectedly obtained as

$$\begin{aligned} \mathbb{E}_\epsilon[\hat{\beta}_{\text{FAB}}] &= \Omega^{-1} \tilde{X}^\top X \beta^* \\ &= \beta^* + \Omega^{-1} \mathbf{b} \end{aligned} \quad (15)$$

for any  $q(Z)$ , where  $\tilde{X} = X \circ M$  and  $b_k = (\mathbf{x}_k \circ \boldsymbol{\mu}_k)^\top \sum_{l \neq k} \beta_l^* (\mathbf{x}_l \circ (\mathbf{1} - \boldsymbol{\mu}_l))$ .

Eq. (15) immediately suggests that  $\hat{\boldsymbol{\beta}}_{\text{FAB}}$  is biased by  $\Omega^{-1}\mathbf{b}$ . The bias consists of the two cross terms:  $(\mathbf{x}_k, \mathbf{x}_l)$  and  $(\boldsymbol{\mu}_k, \mathbf{1} - \boldsymbol{\mu}_l)$ . Thus the bias increases when  $\mathbf{x}_k$  and  $\mathbf{x}_l$  are correlated and  $\mathbf{z}_k$  and  $\mathbf{z}_l$  are negatively correlated. On the other hand, the cross terms become zero when  $\mu_{nk} = 0$  or  $\mu_{nl} = 1$  for all  $n$ . This also implies that the bias is weakened by an appropriately estimated  $q$ . In section 5.2, we numerically evaluate the bias of FAB with Lasso and ARD, showing that FAB achieves the lowest bias.

Remarkably, when  $K = 1$  no cross term appears and the bias is vanished for any  $q$  satisfying  $\pi > 0$ . Also, the 1D estimator is simply written as

$$\hat{\beta}_{\text{FAB}} = \frac{\tilde{\mathbf{x}}^\top \mathbf{y}}{\tilde{\mathbf{x}}^\top \mathbf{x}}. \quad (16)$$

Again, if  $\mu_{nl} = 1$  for all  $n$ ,  $\hat{\beta}_{\text{FAB}}$  recovers  $\hat{\beta}_{\text{LS}}$ .

#### 4.4. The FAB-EG and The Hybrid FAB-EM-EG Algorithms

Hayashi and Fujimaki (2013) reported that model pruning in FAB is slow, and we found that our algorithm shares the same drawback. In our case,  $\{\pi_k\}$  for irrelevant features takes a lot of iterations until the convergence to zero although the weights  $\boldsymbol{\beta}$  and  $\{\pi_k\}$  for relevant features converge rapidly. Below we solve the slow-convergence problem by combining gradient ascent and reparametrization.

First we replaced the FAB-M step by gradient ascent, which was motivated by previous studies (Salakhutdinov et al., 2003; Maeda and Ishii, 2007) that give convergence analysis of the EM algorithm. Then we found that gradient ascent certainly helps; however, the convergence was still slow. This is because the model distribution is insensitive to the direction along with  $\pi_k$  when  $\beta_k$  is small. This means that the gradient for  $\pi_k$  would be shallow for an irrelevant feature  $k$ , since the estimator of  $\beta_k$  takes a small value for the feature.

The natural gradient (NG) method (Amari, 1998) would be effective to overcome the insensitivity in the model distribution. The key idea in NG method is to adopt the Fisher information matrix as a metric on a parameter space (so-called the Fisher information metric), in order to define the distance by the Kullback-Leibler (KL) divergence between model distributions, instead of the Euclidean distance between parameter vectors. Thus, parameter updates by NG method can make steady changes in the model distribution at each iteration. Amari and his co-workers also stated that NG method is especially effective when the parameter space contains singular regions, namely, regions where the Fisher information matrix degenerates (Amari et al., 2006; Wei et al., 2008). That is because the problem of shallow gradient is severe around a singular region, since gradient completely vanishes along with the region. Hence, learning by ordinary gradient is often trapped around singular regions and stays for many iterations, even when the models in the regions show poor agreement with data. In contrast, learning by NG method is free from the slow down.

In our case, the model has two singular regions for each feature, namely,  $\beta_k = 0$  and  $\pi_k = 0$ . In particular, singular region  $\beta_k = 0$  causes the slow convergence. Therefore, NG method should be effective; however, the evaluation of the Fisher information metric is computationally expensive in our case. Then, we instead propose a simple reparametrization that approximates the Fisher information metric. Our strategy is to perform a block

diagonal approximation of the full matrix, as recently done in (Desjardins et al., 2015) for neural networks.

To this end, we examine the Fisher information metric in the single-parameter case ( $K = 1$ ), which approximates diagonal blocks of the full metric. Then the model we concern here is just  $y_n \sim \pi N(y_n|x_n\beta, \lambda^{-1}) + (1 - \pi)N(y_n|0, \lambda^{-1})$ . We focus on the case of small  $\beta$  because the slow learning of  $\pi$  is prominent in this region as noted above. Although the exact form of the metric is still hard to compute, our focus on the small- $\beta$  case allows further approximation. Taylor expansion around  $\beta = 0$  and lowest-order approximation give us a metric tensor:

$$G \equiv \begin{pmatrix} G_{\beta\beta} & G_{\beta\pi} \\ G_{\beta\pi} & G_{\pi\pi} \end{pmatrix} = \lambda N \langle x^2 \rangle \begin{pmatrix} \lambda\beta^2 N \langle x^2 \rangle f(\pi) + \pi^2 & \beta\pi \\ \beta\pi & \beta^2 \end{pmatrix}. \quad (17)$$

where  $f(\pi)$  represent polynomials of  $\pi$  and  $\langle x^2 \rangle \equiv \sum_n x_n^2/N$ . The key factor in  $G$  is  $G_{\pi\pi} \propto \beta^2$  because this represents the fact that smaller value of  $\beta$  makes the model more insensitive to changes in  $\pi$ .

The approximated metric we obtained above is complicated and difficult to handle. Hence we consider the following simple reparametrization for  $k = 1, \dots, K$ :

$$(\beta_k, \pi_k) \rightarrow (\beta_k, s_k = \beta_k \pi_k). \quad (18)$$

Let us show what metric is introduced in  $(\beta, \pi)$ -space through the reparametrization. To this end, we remember that considering usual gradient ascent on  $(\beta, s)$ -space is correspond to introducing a metric  $J^\top J$  in the original space, where  $J$  is the Jacobian matrix for the reparametrization. Then, the reparametrization is correspond to introducing a block diagonal metric tensor in which each diagonal block is

$$G' = \begin{pmatrix} 1 + \pi_k^2 & \beta_k \pi_k \\ \beta_k \pi_k & \beta_k^2 \end{pmatrix}, \quad (19)$$

The similarity between  $G$  and  $G'$  is clear. Although those are not identical,  $G'$  is simpler and shares the key factor as  $G'_{\pi\pi} \propto \beta^2$ .

**FAB-G step** In the FAB-G step, we replace the FAB-M step by gradient ascent. We calculate the gradient on the parameter space after reparametrization  $(\beta_k, s_k)$ , and project it onto the original space. Then we obtain the following update rule for  $(\beta_k, \pi_k)$ :

$$\begin{pmatrix} \beta_k^{t+1} \\ \pi_k^{t+1} \end{pmatrix} = \begin{pmatrix} \beta_k^t \\ \pi_k^t \end{pmatrix} + \eta_t \begin{pmatrix} 1 & -\frac{\pi_k}{\beta_k} \\ -\frac{\pi_k}{\beta_k} & \frac{1+\pi_k^2}{\beta_k^2} \end{pmatrix} \begin{pmatrix} \frac{\partial \mathcal{G}}{\partial \beta_k} \\ \frac{\partial \mathcal{G}}{\partial \pi_k} \end{pmatrix} \quad (20)$$

where  $t$  is the iteration number and  $\{\eta_t\}$  are the learning coefficients. We note that the update of  $\pi_k$  by  $\frac{\partial \mathcal{G}}{\partial \pi_k}$  is scaled by  $\beta_k^{-2}$ , and then accelerated when  $\beta_k$  is small, as expected. When  $\pi_k = 1$ , we update only  $\beta_k$  by  $\eta \frac{\partial \mathcal{G}}{\partial \beta_k}$ . Since the singularity problem comes from  $\beta$  and  $\pi$ , not  $\lambda$ , update of  $\lambda$  remains the closed-form solution eq. (14).

We refer to a FAB algorithm in which the G step replace the M step, as FAB-EG algorithm. Even though the FAB-EG algorithm accelerates the convergence, fast initial progress in the FAB-EM algorithm is still attractive. Then, to receive both benefits, we propose a hybrid algorithm in which the learning progresses by FAB-EM at first and by FAB-EG later. The procedure is shown in the pseudo-code in Algorithm 2.



---

**Algorithm 2** Bayesian masking by Hybrid FAB-EM-EG algorithm

---

```
1: Initialize  $(\{\mu_n\}, \beta, \lambda, \pi)$ 
2:  $t \leftarrow 0$ 
3: repeat
4:   Update  $\{\mu_n\}$  by FAB-E step
5:   for  $k = 1, \dots, K$  do
6:     if  $\sum_n \mu_{nk}/N < \delta$  then
7:       Remove  $k$ -th dimension from the model
8:     end if
9:   end for
10:  if  $t < T$  then
11:    Update  $(\beta, \lambda, \pi)$  by FAB-M step
12:  else
13:    Update  $(\beta, \lambda, \pi)$  by FAB-G step
14:  end if
15:   $t \leftarrow t + 1$ 
16: until termination criterion is met
```

---

## 5. Experiments

### 5.1. Overview

Firstly, in this section, we evaluate BM (our proposed method), Lasso, and ARD with a simple  $K = 2$  example, and show that BM outperforms the others in terms of the sparsity-shrinkage trade-off. Secondly, on the simple example, we also illustrate how the parameters are updated by the FAB-EM and the FAB-EG algorithms, which highlights how the use of gradient ascent and the introduction of the reparametrization avoid being trapped in the singular region. Thirdly, we demonstrate that the Hybrid FAB-EM-EG algorithm converges faster than the FAB-EM algorithm. Lastly, we evaluate BM, Lasso, and ARD again in larger  $K$  examples.

### 5.2. Experiment with Two Features

For demonstration purpose, we borrowed a simple  $K = 2$  setting from [Aravkin et al. \(2014\)](#) who consider

$$\begin{pmatrix} y_1 \\ y_2 \end{pmatrix} = \begin{pmatrix} 1 & 0 \\ 0.5 & 1 \end{pmatrix} \begin{pmatrix} \beta_1 \\ \beta_2 \end{pmatrix} + \begin{pmatrix} \epsilon_1 \\ \epsilon_2 \end{pmatrix} \quad (21)$$

where  $\epsilon_1$  and  $\epsilon_2$  are sampled from  $N(0, 0.005)$ . Assume that the true parameter values are  $\bar{\beta}_1 = 0$  and  $\bar{\beta}_2 = 1$ , i.e., the first feature is irrelevant and the second feature is relevant. Note that the variance is supposed to be known for simplicity.

#### 5.2.1. COMPARISON BETWEEN BM, LASSO, AND ARD

In the setting, we generated 500 datasets; each dataset contains  $2 \times 20$  samples of  $y$ . Note that, in BM (Algorithm 1), we adopted zero tolerance for model pruning—we pruned  $k$ -th

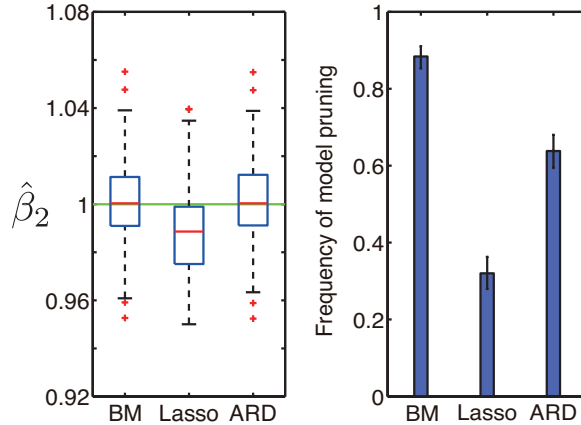


Figure 2: Estimation results on synthetic data from eq. (21). (Left) Box plots of estimated values of  $\beta_2$ . The green line indicates the true value  $\hat{\beta}_2 = 1$ . (Right) Frequency of pruning of the irrelevant feature. The error bars represent 95% confidence interval from fitting of the binomial distribution.

feature only when  $\hat{\pi}_k$  is smaller than machine epsilon. In Lasso, we determined  $\alpha$  by 2-fold cross validation.

The estimation results are summarized in Figure 2; the left panel shows  $\hat{\beta}_2$  in case that the irrelevant feature was pruned and the right panel shows frequency of pruning of the irrelevant feature in the 500 trials. Note that the relevant feature were not pruned in all of the methods. We can easily see that BM achieved the highest sparsity without shrinkage of  $\hat{\beta}_2$ . ARD displayed no visible shrinkage as in BM; however, the sparsity was lower than that of BM. Lasso displayed shrinkage bias and the sparsity was the lowest.

### 5.2.2. LEARNING TRAJECTORY OF THE FAB-EM AND THE FAB-EG ALGORITHMS

On the simple example, we illustrate how the parameters are updated by the FAB-EM and the FAB-EG algorithms. For comparison, we also performed the FAB-EG algorithm without reparametrization. We fixed the learning coefficient as  $\eta_t = 2 \times 10^{-6}$  for FAB-EG and  $= 2 \times 10^{-4}$  for FAB-EG without reparametrization.

Figure 3 shows typical learning trajectories of  $\beta_1$  and  $\pi_1$  with 100 samples. We tried the 10 initial points of  $\beta_1$  and  $\pi_1$  locating diagonally in the upper right. Initial values of  $\beta_2$  and  $\pi_2$  are set to the true values. In FAB-EM, the learning trajectories were trapped around  $\beta_1 = 0$ . In FAB-EG without reparametrization, the trapping was mitigated but still happened especially when the initial values of  $\beta_1$  were small. Intuitively speaking, this is because the gradient for  $\pi_1$  is shallow with small  $\beta_1$ . Hence the learning trajectory approached to smaller  $\beta_1$  since the feature was irrelevant, and then, the learning of  $\pi_1$  became slower. By contrast, the learning trajectories of FAB-EG with the reparametrization approached to  $\pi_1 = 0$  with fewer iterations regardless of the initial points, which means the irrelevant feature was pruned quickly. This result empirically demonstrates that using gradient ascent

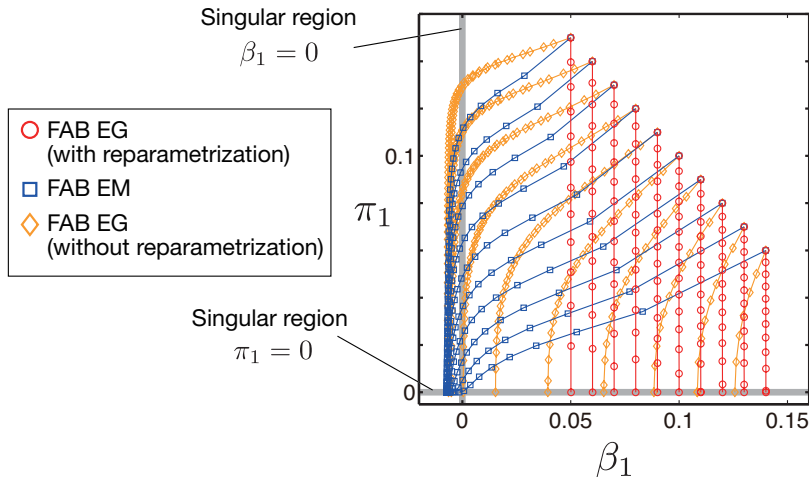


Figure 3: Typical learning trajectories on  $\beta_1$ - $\pi_1$  plane from 10 different initial points by FAB-EM steps and FAB-EG steps with/without reparametrization.

alone improves the convergence a little, but combining with the reparametrization drastically accelerates it.

### 5.3. Experiment with Larger Number of Features

Next, we explain the results with larger examples ( $10 \leq K \leq 50$ ). We generated  $\beta$  and  $X$  from the uniform distribution in  $[0, 1]$  and  $\mathbf{y}$  by eq. (1) with  $\lambda^{-1} = 0.2$ . We set  $N$  to  $20K$ . We controlled  $\{\eta_t\}$  as described in Appendix C.

#### 5.3.1. PERFORMANCE VALIDATION OF THE HYBRID FAB-EM-EG ALGORITHM

With  $K = 50$ , we demonstrate that the Hybrid FAB-EM-EG algorithm converges faster than the FAB-EM algorithm. To this end, we counted number of correctly pruned features, and plotted it against the elapsed time for the algorithms. We set  $T$  in Algorithm 2 to 200 iterations. Figure 4 shows number of correctly pruned features against elapsed time. We can see the faster convergence of the Hybrid FAB-EM-EG algorithm. Note that the faster convergence is not originated from over-pruning because the numbers of wrongly pruned features at the termination were  $2.0 \pm 1.3$  (Hybrid FAB-EM-EG) and  $1.8 \pm 1.3$  (FAB-EM-EG), which were almost the same.

#### 5.3.2. PRECISION AND RECALL

For  $K > 2$  cases, we used two performance measures: Recall and Precision. The measures are defined as Precision =  $m_3/m_2$  and Recall =  $m_3/m_1$  where  $m_1$  and  $m_2$  are the numbers of true and estimated irrelevant features, respectively, and  $m_3$  is the number of correctly pruned features. We examined  $K = 10, 30, 50$ , and for each  $K$ , we generated 50 datasets. Figure 5 summarizes the estimation results from BM (Algorithm 2), Lasso, and ARD. We

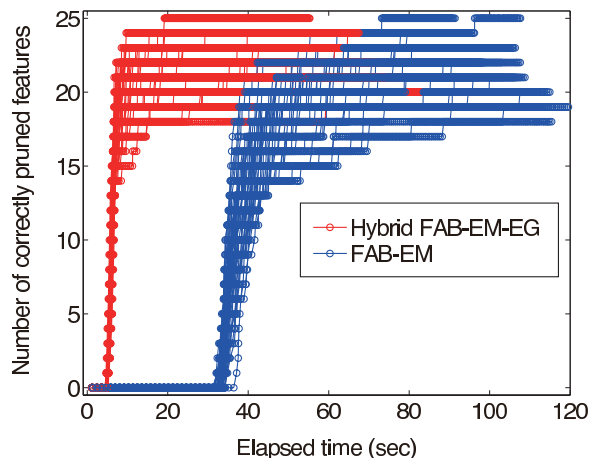


Figure 4: Performance validation of the Hybrid FAB-EM-EG algorithm. For the Hybrid FAB-EM-EG and the FAB-EM algorithms, number of correctly pruned features is plotted against elapsed time. Different lines with the same color represent different datasets.

set  $T$  to 500 iterations. In Lasso,  $\alpha$  was determined by 10-fold cross validation. As shown in the left and middle panels, although BM displayed slightly lower Precision than the others, it achieved the highest Recall. Then we also computed the  $F_1$  score—the harmonic mean of Precision and Recall, which can be interpreted as an evaluation of the performance in terms of the sparsity-shrinkage trade-off. As shown in the right panel, BM attained the highest  $F_1$  score for all  $K$  values in this range. Then we conclude that BM achieved the best performance for the larger  $K$  cases.

## 6. Conclusion

In this paper, we proposed a new sparse estimation method, BM, whose key feature is not to impose direct regularization on the weights. Our strategy was to introduce binary latent variables that randomly mask features and to perform a variational Bayesian inference based on FIC. In addition, we introduced gradient ascent and the reparametrization to accelerate the convergence. Our analysis on the estimators of BM, Lasso, and ARD highlighted how their sparsity mechanisms are different from each other. Experimental comparisons between the methods demonstrated that BM achieves the best performance in terms of the sparsity-shrinkage trade-off.

## References

Shun-ichi Amari. Natural gradient works efficiently in learning. *Neural Computation*, 10: 251–276, 1998.

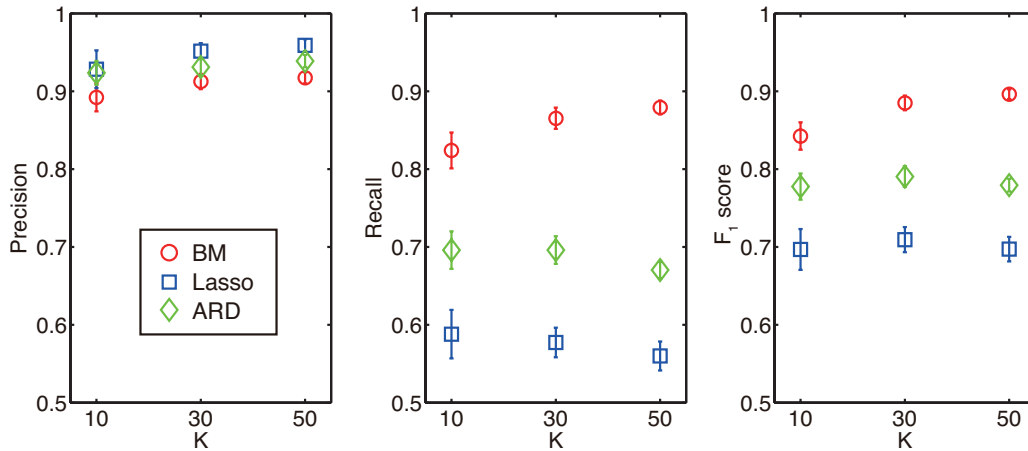


Figure 5: The performance measures are plotted with standard errors. (Left) Precision. (Middle) Recall. (Right) The  $F_1$  score.

Shun-ichi Amari, Hyeyoung Park, and Tomoko Ozeki. Singularities affect dynamics of learning in neuromanifolds. *Neural Computation*, 18(5):1007–1065, 2006.

Aleksandr Aravkin, James V. Burke, Alessandro Chiuso, and Gianluigi Pillonetto. Convex vs non-convex estimators for regression and sparse estimation: the mean squared error properties of ARD and GLasso. *Journal of Machine Learning Research*, 15:217–252, 2014.

G. Desjardins, K. Simonyan, R. Pascanu, and K. Kavukcuoglu. Natural Neural Networks. *ArXiv e-prints*, 2015.

Ryohei Fujimaki and Satoshi Morinaga. Factorized asymptotic bayesian inference for mixture modeling. In *AISTATS*, 2012.

Kohei Hayashi and Ryohei Fujimaki. Factorized asymptotic bayesian inference for latent feature models. In *27th Annual Conference on Neural Information Processing Systems (NIPS)*, 2013.

Kohei Hayashi, Shin-ishi Maeda, and Ryohei Fujimaki. Rebuilding factorized information criterion: Asymptotically accurate marginal likelihood. In *International Conference on Machine Learning (ICML)*, 2015.

DavidJ MacKay. Bayesian Methods for Backpropagation Networks. In *Models of Neural Networks III*, pages 211–254. Springer, 1994.

Shin-ichi Maeda and Shin Ishii. Convergence analysis of the EM algorithm and joint minimization of free energy. In *IEEE Workshop on Machine Learning for Signal Processing*, 2007.

Radford M. Neal. *Bayesian Learning for Neural Networks*. Springer, 1996.

K. B. Petersen and M. S. Pedersen. The matrix cookbook, 2012.

Ruslan Salakhutdinov, Sam Roweis, and Zoubin Ghahramani. Optimization with EM and expectation-conjugate-gradient. In *International Conference on Machine Learning (ICML)*, 2003.

Robert Tibshirani. Regression shrinkage and selection via the lasso. *Journal of the Royal Statistical Society, Series B*, 58:267–288, 1994.

Haikun Wei, Jun Zhang, Florent Cousseau, Tomoko Ozeki, and Shun-ichi Amari. Dynamics of learning near singularities in layered networks. *Neural Computation*, 20(3):813–843, 2008.

David P. Wipf and Srikantan S. Nagarajan. A new view of automatic relevance determination. In *Advances in Neural Information Processing Systems 20*, 2008.

## Appendix A. The One-Dimensional ARD Estimator

According to [Wipf and Nagarajan \(2008\)](#), the negative marginal log-likelihood when  $K = 1$  is given by

$$\log |\lambda^{-1}I + \gamma \mathbf{x} \mathbf{x}^\top| + \mathbf{y}^\top (\lambda^{-1}I + \gamma \mathbf{x} \mathbf{x}^\top)^{-1} \mathbf{y} \quad (22)$$

$$= \log(\lambda^{-1} + \gamma \mathbf{x}^\top \mathbf{x}) + \lambda \mathbf{y}^\top \mathbf{y} - \mathbf{y}^\top \frac{\lambda^2 \gamma \mathbf{x} \mathbf{x}^\top}{1 + \lambda \gamma \mathbf{x}^\top \mathbf{x}} \mathbf{y} \quad (23)$$

$$= \log(\lambda^{-1} + \gamma \mathbf{x}^\top \mathbf{x}) + \lambda \mathbf{y}^\top \mathbf{y} - \frac{\lambda \gamma (\mathbf{x}^\top \mathbf{y})^2}{\lambda^{-1} + \gamma \mathbf{x}^\top \mathbf{x}} \quad (24)$$

In the second line we use the matrix determinant lemma ([Petersen and Pedersen, 2012](#), eq. (24)) for the first term and the variant of the Sherman-Morrison relation ([Petersen and Pedersen, 2012](#), eq. (160)) for the second term. The derivative is

$$\frac{\partial \text{eq. (24)}}{\partial \gamma} = \frac{\mathbf{x}^\top \mathbf{x}}{\lambda^{-1} + \gamma \mathbf{x}^\top \mathbf{x}} - \frac{\lambda (\mathbf{x}^\top \mathbf{y})^2}{\lambda^{-1} + \gamma \mathbf{x}^\top \mathbf{x}} + \frac{\lambda \gamma (\mathbf{x}^\top \mathbf{y})^2 \mathbf{x}^\top \mathbf{x}}{(\lambda^{-1} + \gamma \mathbf{x}^\top \mathbf{x})^2} \quad (25)$$

$$= \frac{\mathbf{x}^\top \mathbf{x} (\lambda^{-1} + \gamma \mathbf{x}^\top \mathbf{x}) - \lambda (\mathbf{x}^\top \mathbf{y})^2 (\lambda^{-1} + \gamma \mathbf{x}^\top \mathbf{x}) + \lambda \gamma (\mathbf{x}^\top \mathbf{y})^2 \mathbf{x}^\top \mathbf{x}}{(\lambda^{-1} + \gamma \mathbf{x}^\top \mathbf{x})^2} \quad (26)$$

$$= \frac{\lambda^{-1} \mathbf{x}^\top \mathbf{x} + \gamma (\mathbf{x}^\top \mathbf{x})^2 - (\mathbf{x}^\top \mathbf{y})^2}{(\lambda^{-1} + \gamma \mathbf{x}^\top \mathbf{x})^2} \quad (27)$$

The stationary point is then given as

$$\hat{\gamma} = \max\left(0, \frac{(\mathbf{x}^\top \mathbf{y})^2 - \lambda^{-1} \mathbf{x}^\top \mathbf{x}}{(\mathbf{x}^\top \mathbf{x})^2}\right) \quad (28)$$

$$= \max\left(0, \hat{\beta}_{\text{LS}}^2 - (\lambda \mathbf{x}^\top \mathbf{x})^{-1}\right). \quad (29)$$

Note that, we put the max operator since  $\gamma$  is the variance and it must be non-negative. By putting the result of  $\hat{\gamma} > 0$  into eq. (5), we obtain

$$\hat{\beta}_{\text{ARD}} = \hat{\gamma} \mathbf{x}^\top (\lambda^{-1} I + \hat{\gamma} \mathbf{x} \mathbf{x}^\top)^{-1} \mathbf{y} \quad (30)$$

$$= \lambda \hat{\gamma} \mathbf{x}^\top \mathbf{y} - \frac{\lambda \hat{\gamma}^2 \mathbf{x}^\top \mathbf{x} \mathbf{x}^\top \mathbf{y}}{\lambda^{-1} + \hat{\gamma} \mathbf{x}^\top \mathbf{x}} \quad (31)$$

$$= \lambda \hat{\beta}_{\text{LS}}^2 \mathbf{x}^\top \mathbf{y} - \hat{\beta}_{\text{LS}} - \frac{\lambda \hat{\beta}_{\text{LS}}^4 \mathbf{x}^\top \mathbf{x} \mathbf{x}^\top \mathbf{y} - 2 \hat{\beta}_{\text{LS}}^2 \mathbf{x}^\top \mathbf{y} + \frac{\lambda \mathbf{x}^\top \mathbf{y}}{\lambda^2 \mathbf{x}^\top \mathbf{x}}}{\lambda^{-1} + \hat{\beta}_{\text{LS}}^2 \mathbf{x}^\top \mathbf{x} - \lambda^{-1}} \quad (32)$$

$$= \lambda \hat{\beta}_{\text{LS}}^2 \mathbf{x}^\top \mathbf{y} - \hat{\beta}_{\text{LS}} - \frac{\lambda \hat{\beta}_{\text{LS}}^4 \mathbf{x}^\top \mathbf{x} \mathbf{x}^\top \mathbf{y} - 2 \hat{\beta}_{\text{LS}}^2 \mathbf{x}^\top \mathbf{y} + \lambda^{-1} \hat{\beta}_{\text{LS}}}{\hat{\beta}_{\text{LS}}^2 \mathbf{x}^\top \mathbf{x}} \quad (33)$$

$$= -\hat{\beta}_{\text{LS}} + 2 \hat{\beta}_{\text{LS}} - \frac{1}{\lambda \hat{\beta}_{\text{LS}} \mathbf{x}^\top \mathbf{x}} \quad (34)$$

$$= \hat{\beta}_{\text{LS}} - \frac{1}{\lambda \mathbf{x}^\top \mathbf{y}}. \quad (35)$$

Recall  $\hat{\beta}_{\text{ARD}} = 0$  when  $\hat{\gamma} \leq 0$ . Since  $\hat{\beta}_{\text{LS}}^2$  and  $(\lambda \mathbf{x}^\top \mathbf{x})^{-1}$  are both non-negative, the condition  $\hat{\gamma} \leq 0$  is written as  $\hat{\beta}_{\text{LS}}^2 \leq (\lambda \mathbf{x}^\top \mathbf{x})^{-1}$  or equivalently  $|\hat{\beta}_{\text{LS}}| \leq |\lambda \mathbf{x}^\top \mathbf{y}|^{-1}$ . Substituting this condition into the above equation yields eq. (8).

## Appendix B. Derivation of The Lower Bound of FIC

Hayashi et al. (2015) give us a general representation of a lower bound of FIC, and in this case, we have

$$\text{FIC} \geq \mathbb{E}_q[\log p(\mathbf{y}, Z|X, \boldsymbol{\beta}, \lambda, \boldsymbol{\pi})] - \frac{1}{2} \mathbb{E}_q[\log |F_{\boldsymbol{\beta}}|] - \frac{K+1}{2} \log N + H(q). \quad (36)$$

where  $q = q(Z)$  and  $F_{\boldsymbol{\beta}}$  means the Hessian matrix of the negative log-likelihood w.r.t.  $\boldsymbol{\beta}$ . Note that the priors for  $\boldsymbol{\beta}$  and  $\lambda$  do not appear in the lower bound, since the priors do not depend on  $N$  as assumed in section 4.1. In order to derive a FAB algorithm, we compute a lower bound of the second term in RHS.

The Hessian matrix  $F_{\boldsymbol{\beta}}$  is represented as

$$F_{\boldsymbol{\beta}} = -\nabla_{\boldsymbol{\beta}} \nabla_{\boldsymbol{\beta}} \log p(\mathbf{y}, Z|X, \boldsymbol{\beta}, \lambda, \boldsymbol{\pi}) \quad (37)$$

$$= (X \circ Z)^\top (X \circ Z). \quad (38)$$

Then, use of Hadamard's inequality for a positive-semidefinite matrix yields

$$-\log |F_{\boldsymbol{\beta}}| \geq -\sum_k \log \sum_n x_{nk}^2 z_{nk} \quad (39)$$

$$\geq -\sum_k \log \left( \sum_n z_{nk} \right) \left( \sum_n x_{nk}^2 \right) \quad (40)$$

$$= -\sum_k \log \sum_n z_{nk} + \text{const.} \quad (41)$$

As stated in [Fujimaki and Morinaga \(2012\)](#), since  $-\log \sum_n z_{nk}$  is a concave function, its linear approximation at  $N\pi_k > 0$  yields the lower-bound:

$$-\mathbb{E}_q[\log \sum_n z_{nk}] \geq -\left(\log N\pi_k + \frac{\sum_n \mathbb{E}_q[z_{nk}]/N - \pi_k}{\pi_k}\right). \quad (42)$$

Therefore, we obtain eq. (10) in the maintext.

### Appendix C. Control of Learning Coefficient

We explain how to set the learning coefficients  $\{\eta_t\}$  in section 5.3. We set  $\eta_t$  to a constant value  $\eta$ ; however, when maximum of the update of  $\{\pi_k\}$  is greater than 0.05,  $\eta_t$  is modified so that the maximum is 0.05. We chose the constant  $\eta$  as  $2 \times 10^{-2}/N$  where  $N$  is number of samples.